RSC Advances

PAPER

View Article Online
View Journal | View Issue

Cite this: *RSC Adv.*, 2018, **8**, 33398

Efficient alkaloid capture from water using a charged porous organic polymer†

Qing-Mei Zhang,[a] Zhen Wang,[a] Guang Cheng,[b] Hui Ma,[a] Qing-Pu Zhang,[a] Fu-Xian Wan,[d] Bien Tan[b] and Chun Zhang *[ac]

Received 2nd August 2018
Accepted 20th September 2018

DOI: 10.1039/c8ra06499g

rsc.li/rsc-advances

Berberine hydrochloride (BH), an important alkaloid, can be captured from water and released in organic solution circularly by a charged porous polymer (TPB–HCP), which is hypercross-linked using the cost-effective Friedel–Crafts reaction using sodium tetraphenylborate as the monomer. With high BET surface area, hierarchical porous structure and charged characteristics, TPB–HCP displays excellent adsorption capacity for BH owing to the synergistic effects of size matching and electrostatic interaction.

Introduction

Alkaloids, a class of naturally occurring nitrogen-containing compounds, display a wide range of pharmacological activities against many diseases including cancer,[1] gastroenteritis,[2] obesity[3] and so on. Generally, the alkaloids' purification from crude extracts or recycling from waste water is carried out by acid–base extraction.[4] However, the extensive use of inorganic acids and bases will undoubtedly increase the risk of environmental pollution and increase their cost of production. Using porous materials as adsorbents to enrich or recycle alkaloids from crude extracts or waste water might be a cost-effective means to avoid the use of acid and base.

Compared with the traditional inorganic porous materials (active carbon,[5] zeolites[6] and molecular sieves[7]) with shortcoming of instability, low surface area and low adsorption capacity, porous organic polymers (POPs)[8] exhibit many advantages including high surface area, easy functionality and fine stability. Among different POPs, hyper cross-linked polymers (HCPs) [9–11] attracted great attentions because of their characteristics of low-cost and easy synthesis. Especially, Tan and co-operators recently developed a cost-effective knitting strategy by Friedel–Crafts reaction to prepare HCPs.[12] Recently, three-dimensional rigid building blocks had been used to construct HCPs successfully for enhancing their porous properties.[13–15] Although HCPs based three-dimensional rigid monomers could enhance the interaction with guests, these HCPs frameworks mainly relied on neutral monomers.[16] Then integration of charged blocks into the networks makes that HCPs apply in more areas probably.[17] On the one hand, charged HCPs as adsorbents might be feasible to strengthen adsorption capacity owing to electrostatic interaction.

Tetraphenylborate sodium, is an interesting ionic salt with three-dimensional rigid structure. Some charged POPs based tetraphenylborate ions were developed successfully and applied in fields of catalysts, adsorptions, and energy storage and conversions.[18,19] For examples, Long and coworkers developed tetraarylborate polymer networks for solid electrolytes.[20] Zhu's groups reported several charged porous aromatic frameworks for iodine adsorption.[21] As early as 1968, Ebel found that tetraphenylborate sodium could be used to titrate alkaloids in water solution by precipitation method.[22] Inspired by these interesting results, we speculated that cross-linking tetraphenylborate sodium into porous networks might provide new opportunities in the field of alkaloids adsorption because of their charged networks and the 3D rigid structure.

Herein, we cross-linked tetraphenylborate sodium using formaldehyde dimethyl acetal (FDA) as cross-linker and prepared a tetraphenylborate sodium-based HCPs (TPB–HCP). The charged TPB–HCP not only displayed high surface area and good stability, but also had excellent adsorption ability for berberine hydrochloride, a class of important alkaloid, from aqueous solution.

Results and discussion

The synthesis of TPB–HCP was described in Scheme 1. Typically, tetraphenylboron sodium was polymerized with FDA in 1,2-dichloroethane, promoting by anhydrous $FeCl_3$. The resulted brown power (TPB–HCP) with yield of 75% was found to be insoluble in any common organic solvents.

[a]College of Life Science and Technology National Engineering Research Center for Nanomedicine, Huazhong University of Science and Technology, Wuhan 430074, China. E-mail: chunzhang@hust.edu.cn

[b]School of Chemistry and Chemical Engineering, Huazhong University of Science and Technology, Wuhan 430074, China. E-mail: bien.tan@mail.hust.edu.cn

[c]College of Chemistry and Molecular Engineering, Qingdao University of Science and Technology, Qingdao, 266042, China

[d]College of Chemistry and Material Science, Shandong Agricultural University, Taian 271018, China

† Electronic supplementary information (ESI) available: FT-IR, XRD, TGA of TPB–HCP, molecular sizes of BH, UV-vis adsorption spectra and the Langmuir isotherm model of CV, CR and MB. See DOI: 10.1039/c8ra06499g

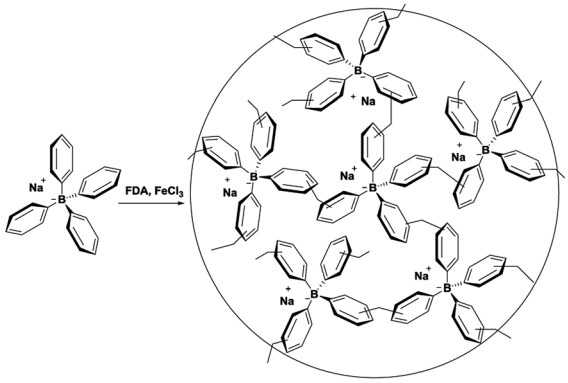

Scheme 1 Synthesis of TPB–HCP. Reagents and conditions: FDA, $FeCl_3$, 1,2-dichloroethane, 80 °C, 72 h.

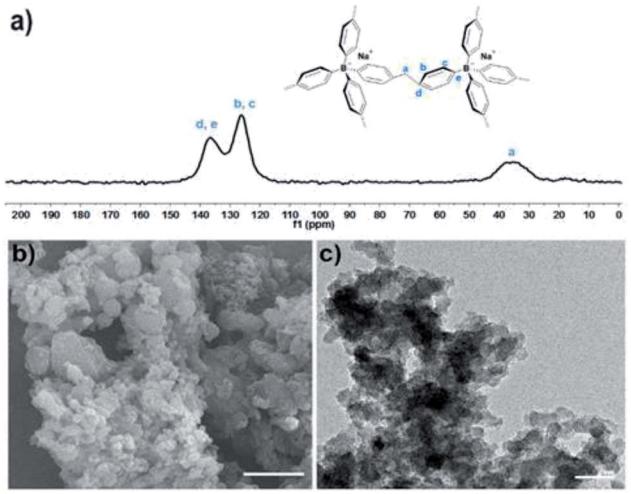

Fig. 1 (a) Cross-polarization (CP) ^{13}C MAS NMR spectrum of TPB–HCP. (b) SEM and (c) TEM of TPB–HCP. Scale bar: 1 μm (a) and 200 nm (b).

The structure of TPB–HCP was confirmed by FT-IR and cross-polarization (CP) ^{13}C MAS NMR experiment. The bands at 2853 and 2900 cm^{-1} were observed in FT-IR spectrum, which was corresponded to the vibrations of methylene bands (ESI, Fig. S1†). For cross-polarization (CP) ^{13}C MAS NMR experiment, three different resonance peaks near 35, 124 and 136 ppm was consistent of the methylene carbon (a), the aromatic carbons (b and c) and the aromatic carbons (d and e), respectively (Fig. 1a). Hence, the successful formation of TPB–HCP was demonstrated by FT-IR and ^{13}C MAS NMR. The morphology of TPB–HCP was investigated by FE-SEM (Fig. 1b) and TEM (Fig. 1c), it was showed that TPB–HCP adopted an irregular sphere structure. Powder X-ray diffraction (XRD) spectrum displayed broad peaks and also illustrated TPB–HCP's uniform characteristic, as shown in Fig. S2 (ESI†). The result of thermogravimetric analysis (TGA) showed that TPB–HCP had high thermal stability, the material could be stable up to near 400 °C under N_2 atmosphere (ESI, Fig. S3†). Besides, TPB–HCP displayed a distinct negative zeta potential (−18 mV).

Porous characteristics of TPB–HCP were measured by N_2 adsorption–desorption isotherm at 77 K (Fig. 2a). The BET

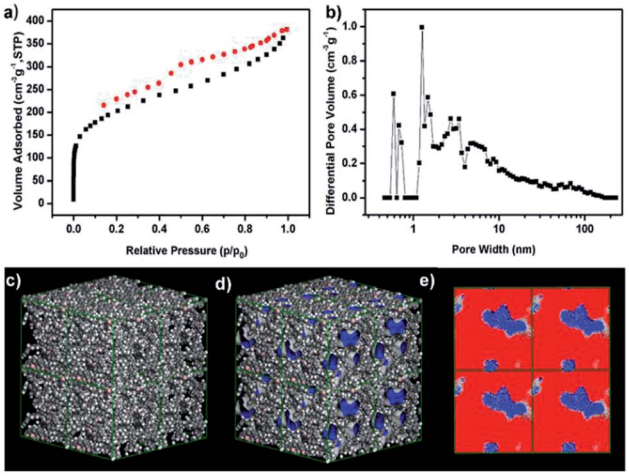

Fig. 2 (a) Nitrogen sorption isotherm at 77 K, black symbols denote gas adsorption, and red symbols denote gas desorption. (b) Pore size distribution calculated using NLDFT method of TPB–HCP. (c) Simulated TPB–HCP dimension of simulation box (the "amorphous cell") = 3.292 nm. Carbon atom was grey and hydrogen atom was white. (d) Three-dimensional array of eight (2 × 2 × 2) amorphous cells with periodic boundary conditions, A Connolly surface was shown in blue/grey. Connolly surface area = 964 m^2 g^{-1}, simulated micropore volume = 0.12 cm^3 g^{-1}. (e) Two-dimensional "slice" through the simulated pore structure. The occupied and unoccupied volume is shown in red and blue, respectively.

surface area of TPB–HCP was calculated to be 717 m^2 g^{-1} (Langmuir surface area was 984 m^2 g^{-1}). For N_2 sorption isotherms of TPB–HCP, a type I adsorption curve was observed, a steep gas uptake at low relative pressure (P/P_0 < 0.001) reflected the existence of abundant micropores. A rise at the medium- and high-pressure region (P/P_0 = 0.8–1.0) indicated the presence of macropores in the TPB–HCP networks. The hysteresis hoop was measured in the isotherm curves, and this phenomenon was related to irreversible uptake of gas molecules in the pores, which was probably due to network swelling. By using Non-Local Density Functional Theory (NLDFT) method, the pore size distribution of TPB–HCP also confirmed the presence of primary micropore and a spot of meso- and macropore (Fig. 2b). Atomistic simulation[11] results of TPB–HCP were shown (Fig. 2c–e). The Connolly surface area of TPB–HCP was 964 m^2 g^{-1}, and higher than experimental BET surface value (717 m^2 g^{-1}), which was assigned to no permanent interconnected pore structure for TPB–HCP.[23] Moreover, a two-dimensional "slice" through the simulated pore structure was showed, the model simulated the pore micropore dimensions of TPB–HCP quite well (Fig. 2e).

Given the hierarchical porous and charged structure of TPB–HCP, we attempted to use TPB–HCP as adsorbents to capture some important bioactive substances like alkaloids. Berberine, a kind of important alkaloids, have prominent pharmacological activities on gastrointestinal remedy.[24] To evaluate the adsorption capability of TPB–HCP, UV-visible (UV-vis) spectra experiments of berberine hydrochloride (BH) (Fig. 3a) were conducted. More than 99% of BH was removed at room temperature within 5 minutes (Fig. 3b and c). To further

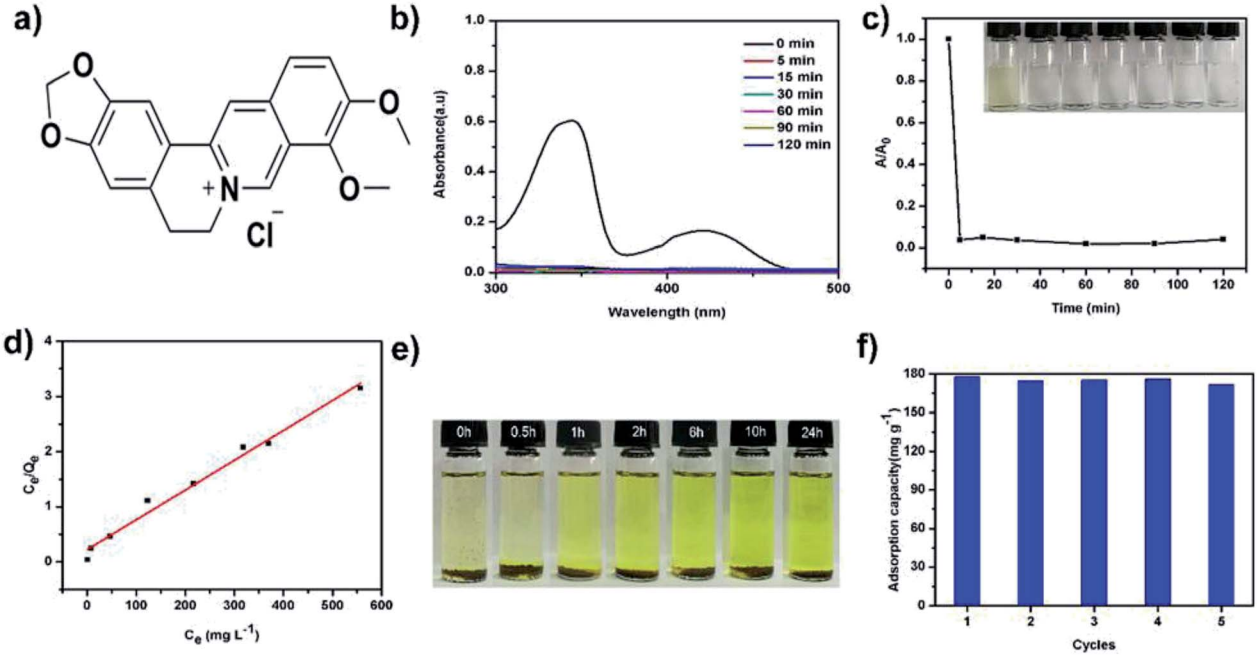

Fig. 3 (a) The structure of berberine hydrochloride. (b) UV-vis adsorption spectra of the aqueous solutions of berberine hydrochloride in the presence of TPB–HCP at different intervals. (c) Adsorption rates of berberine hydrochloride, the initial concentration of berberine hydrochloride solution is 10 mg L^{-1}. (d) The Langmuir isotherm model for berberine hydrochloride on TPB–HCP. (e) Photographs showing the color changes about berberine hydrochloride released experiment. (f) The cycle experiment of TPB–HCP.

investigate the adsorption behaviour of TPB–HCP, the Langmuir isotherm model was used to fit the equilibrium data of adsorption (Fig. 3d). For BH, the correlation coefficient of Langmuir isotherm model (R_L^2) was 0.983 and suggested that the adsorption process followed Langmuir isotherm model (ESI, Table S1†). Fitted by this model, the maximum adsorption capacities of TPB–HCP for BH was thus calculated as 185 mg g^{-1}. In comparison, the commercial activated carbon (granular active charcoal) displayed 180 mg g^{-1} BH uptake capability under the same conditions as almost same as that of TPB–HCP (ESI, Fig. S7†). Although TPB–HCP is no superior to activated carbon for BH adsorption obviously, we think, it is meaningful that alkaloids could be recycled in the adsorption and desorption process of charged porous organic polymers. Compared with acid–base extractions, this adsorption method is more low-cost and environmental friendly. This may provide new ideas for solving other alkaloids or similar drugs problems by means of chemical materials. To understand the adsorption process, we estimated the diameter of BH molecule by MM2 and calculated the size of 15.0 Å (ESI, Fig. S4†). Considering abundant micropores (≤2 nm) in TPB–HCP scaffold and the electrostatic interaction between TPB–HCP with BH, we speculated BH could enter into networks of TPB–HCP, and the adsorption process was homogeneous, which was consistent with the Langmuir model. The high capacity with fast adsorption kinetics implies that TPB–HCP is highly competitive as an effective adsorbent for the capture of BH from water. In brief, TPB–HCP shows good uptake of alkaloids like BH, because of its higher surface area, hierarchical porosity and electrostatic interactions, which ensures high uptake of alkaloids by adsorption and hierarchical pore filling.

Moreover, the BH adsorption of TPB–HCP is reversible. The captured BH can be released from charged polymer networks by immersing the BH-loaded TPB–HCP in ethanol at room temperature. With prolonged release time, the color of the solution changed from colorless to dark yellow, which indicated that TPB–HCP could be regenerated easily in the process of delivering alkaloids (Fig. 3e). So, to prove this, we researched the cycling performance of TPB–HCP for BH sorption. In that case, BH-loaded TPB–HCP was washed until the filtrate was colorless and subsequent TPB–HCP was dried in vacuum for the next BH adsorption cycle. TPB–HCP displayed almost the same property after five cycles, which confirmed TPB–HCP was stable in the process of adsorbing BH circularly (Fig. 3f).

We had also investigated the adsorption capacities of TPB–HCP for BH under different pH conditions. Compared to other pH conditions, the adsorption capacity of TPB–HCP for BH was increased at pH value of 13 (ESI, Fig. S8†), this phenomenon may be due to the free base formation of BH under strong alkaline conditions, which made that TPB–HCP was easier to combine with BH to increase adsorption capacity. On the other hand, in order to investigate the effect of salt on the adsorption of BH by TPB–HCP, different concentrations of NaCl was chosen to adjust ionic strength. It's can be seen that the adsorption capacities of BH on TPB–HCP were decreased as the concentrations of NaCl increased (ESI, Fig. S9†). This indicated that the adsorption of BH on TPB–HCP was affected by ionic strength. These results reveal that electrostatic interaction is one of

possible mechanisms in the adsorption process of BH on TPB–HCP.

In addition to BH, we evaluated the ability of TPB–HCP to remove organic dyes including Crystal Violet (CV), Congo Red (CR), and Methyl Blue (MB) with different size and charge performance. UV-vis spectra experiments displayed that all three kinds of dyes could be removed from water within 5 min by TPB–HCP (ESI, Fig. S5†). Fitting by Langmuir isotherm model (ESI, Fig. S6†), the maximum adsorption values of CV, CR, and MB were calculated as 274, 243 and 146 mg g^{-1}, respectively (ESI, Table S1†). For CV, the kind of cationic dyes could be combined with anionic materials by electrostatic interaction and increased adsorption value, which might be the reason that its adsorption value was higher than that of other anionic dyes (CR and MB).

Conclusions

In summary, a tetraphenylborate sodium-based charged hyper cross-linked polymer (TPB–HCP) was successfully synthesized by low-cost Friedel–Crafts alkylation reaction. With high BET surface area, hierarchical porous structure and charged character, TPB–HCP displayed excellent reversible adsorption for berberine hydrochloride and other cation organic dyes from water, in which synergistic effects of simple physical adsorption and electrostatic interaction might play a very important role. These results demonstrate that TPB–HCP might be an ideal adsorbent for a wide range of large-scale applications in alkaloids extraction or recovery.

Experimental section

Synthesis of TPB–HCP

Tetraphenylboron sodium (1.71 g, 5 mmol) and 4.0 equiv. of FDA (1.52 g, 20 mmol) and 4.0 equiv. of $FeCl_3$ (3.24 g, 20 mmol) were dissolved in 20 mL DCE in the 100 mL round-bottom flask, then heated to 80 °C for 72 h. After reaction, the mixture was filtrated several times with methanol, then purified by Soxhlet extraction with methanol for 48 h, dried in the vacuum for 24 h at 60 °C, finally brown powder was obtained, the yield of which is about 75%.

Atomistic simulation

The model of TPB–HCP was constructed using Material Studio 4.3 to describe the structure of TPB–HCP network. The model was constructed from a combination clusters containing 174 carbon atoms. First, each cluster was fully relaxed using the Discover module and the COMPASS force field, to ensure the cell parameters and hence the density remained constant, the models were again fully relaxed the Discover module and the COMPASS force field. A Connolly surface was created for model using atom, volumes and surface tool in Materials Studio using a fine grid resolution (0.4 Å) and a Connolly radius set to 1.82 Å (the kinetic radius of N_2). The models simulated the pore dimensions of TPB–HCP; the majority of the pore channels in width were 3–20 Å for TPB–HCP.

Berberine hydrochloride and dye adsorption tests

BH, CV, CR and MB were used in this study. In a typical adsorption kinetics of BH experiment, 10 mg TPB–HCP was added to 4 mL of BH aqueous solution (10 mg L^{-1}), then stirred magnetically. The mixture was separated by centrifugation at different time points, 10 000 rpm, ten minutes, two times; then UV-vis spectra were measured. For adsorption capacity experiment, the initial berberine hydrochloride concentration was varied from 50 to 1000 mg L^{-1}, and the mixture was stirred overnight to obtain the adsorption isotherm. The adsorption study of CV, CR and MB was similar to that of BH except the different concentration of aqueous solution used (CV, CR, MB: 10 mg L^{-1}, 50 mg L^{-1},10 mg L^{-1}) for the adsorption experiment and from 50 to 1600 mg L^{-1} for the adsorption isotherm experiment. The adsorption isotherms were fitted by using the Langmuir model. The linear formula of Langmuir isotherm model could be expressed as follows:

$$C_e/Q_e = 1/(K_L Q_m) + C_e/Q_m$$

in which C_e (mg L^{-1}) denotes the equilibrium concentration, Q_e (mg g^{-1}) denotes the equilibrium adsorption capacity, Q_m (mg g^{-1}) denotes maximum adsorption capacity, K_L denotes the Langmuir constant.

Berberine hydrochloride adsorption tests under different PH and NaCl solutions

10 mg TPB–HCP was added to 25 mL of BH aqueous solution (100 mg L^{-1}) at PH values of 2 to 13, the mixture was stirred magnetically overnight. Then the mixture was separated by centrifugation of 10 000 rpm, ten minutes, two times; UV-vis spectra were measured. For NaCl, the study was similar to that of PH except the concentration from 0.02 to 0.08 mol L^{-1}.

Conflicts of interest

There are no conflicts to declare.

Acknowledgements

This work is supported by the National Natural Science Foundation of China (21672078 and 21875079), the Natural Science Foundation of Hubei Province (2016CFB372), and the Applied Basic Research Program of Wuhan City (2016010101010017). We thank the Analytical and Testing Center of Huazhong University of Science and Technology for related analysis.

References

1 (*a*) M. A. Jordan and L. Wilson, *Nat. Rev. Cancer*, 2004, **4**, 253; (*b*) K. Yamamoto, K. Takahashi, H. Mizuno, A. Anegawa, K. Ishizaki, H. Fukaki, M. Ohnishi, M. Yamazaki, T. Masujima and T. Mimura, *Proc. Natl. Acad. Sci. U. S. A.*, 2016, **113**, 3891.

2 Y.-X. Sun, M.-F. Xia, H.-M. Yan, Y.-M. Han, F.-F. Zhang, Z.-M. Hu, A.-Y. Cui, F.-G. Ma, Z.-S. Liu, Q. Gong,

X.-Q. Chen, J. Gao, H. Bian, Y. Tan, Y. Li and X. Gao, *Br. J. Pharmacol.*, 2018, **175**, 374.

3 Y. S. Lee, W. S. Kim, K. H. Kim, M. J. Yoon, H. J. Cho, Y. Shen, J. M. Ye, C. H. Lee, W. K. Oh, C. T. Kim, C. Hohnen-Behrens, A. Gosby, E. W. Kraegen, D. E. James and J. B. Kim, *Diabetes*, 2006, **55**, 2256.

4 L.-F. Jiang, B.-C. Chen, B. Chen, X.-J. Li, H.-L. Liao, W.-Y. Zhang and L. Wu, *J. Sep. Sci.*, 2017, **40**, 2933.

5 A. Bhatnagar, W. Hogland, M. Marques and M. Sillanpää, *Chem. Eng. J.*, 2013, **219**, 499.

6 M. Minceva, R. Fajgar, L. Markovska and V. Meshko, *Sep. Sci. Technol.*, 2008, **43**, 2117.

7 K. W. Chapman, P. J. Chupas and T. M. Nenoff, *J. Am. Chem. Soc.*, 2010, **132**, 8897.

8 (*a*) S. Das, P. Heasman, T. Ben and S.-L. Qiu, *Chem. Rev.*, 2017, **117**, 1515; (*b*) A. Alsbaiee, B. J. Smith, L.-L. Xiao, Y.-H. Ling, D. E. Helbling and W. R. Dichtel, *Nature*, 2016, **529**, 190; (*c*) R. Dawson, A. I. Cooper and D. J. Adams, *Prog. Polym. Sci.*, 2012, **37**, 530.

9 L.-X. Tan and B. Tan, *Chem. Soc. Rev.*, 2017, **46**, 3322.

10 C. D. Wood, B. Tan, A. Trewin, H.-J. Niu, D. Bradshaw, M. J. Rosseinsky, Y. Z. Khimyak, N. L. Campbell, R. Kirk, E. Stocher and A. I. Cooper, *Chem. Mater.*, 2007, **19**, 2034.

11 (*a*) T.-L. Zhai, L. Tan, Y. Luo, J.-M. Liu, B. Tan, X.-L. Yang, H.-B. Xu and C. Zhang, *Chem.–Asian J.*, 2016, **11**, 294; (*b*) C. Zhang, P.-C. Zhu, L. Tan, L.-N. Luo, Y. Liu, J.-M. Liu, S.-Y. Ding, B. Tan, X.-L. Yang and H.-B. Xu, *Polymer*, 2016, **82**, 100; (*c*) J.-S. M. Lee, M. E. Briggs, T. Hasell and A. I. Cooper, *Adv. Mater.*, 2016, **28**, 9804.

12 (*a*) B. Li, R. Gong, W. Wang, X. Huang, W. Zhang, H. Li, C. Hu and B. Tan, *Macromolecules*, 2011, **44**, 2410; (*b*) Y. Luo, B. Li, W. Wang, K. Wu and B. Tan, *Adv. Mater.*, 2012, **24**, 5703; (*c*) B. Li, Z. Guan, W. Wang, X. Yang, J. Hu, B. Tan and T. Li, *Adv. Mater.*, 2012, **24**, 3390.

13 C. Zhang, P.-C. Zhu, L.-X. Tan, J.-M. Liu, B. Tan, X.-L. Yang and H.-B. Xu, *Macromolecules*, 2015, **48**, 8509.

14 (*a*) R. Dawson, L. A. Stevens, T. C. Drage, C. E. Snape, M. W. Smith, D. J. Adams and A. I. Cooper, *J. Am. Chem. Soc.*, 2012, **134**, 10741; (*b*) R. Dawson, E. Stockel, J. R. Holst, D. J. Adams and A. I. Cooper, *Energy Environ. Sci.*, 2011, **4**, 4239.

15 Z. Qiao, S. Chai, K. Nelson, Z. Bi, J. Chen, S. M. Mahurin, X. Zhu and S. Dai, *Nat. Commun.*, 2014, **5**, 3705.

16 (*a*) J.-K. Sun, M. Antonietti and J.-Y. Yuan, *Chem. Soc. Rev.*, 2016, **45**, 6627; (*b*) J. Tian, T.-Y. Zhou, S.-C. Zhang, S. Aloni, M. V. Altoe, S.-H. Xie, H. Wang, D.-W. Zhang, X. Zhao, Y. Liu and Z.-T. Li, *Nat. Commun.*, 2014, **5**, 1.

17 (*a*) S. Hao, Y.-C. Liu, C.-N. Shang, Z.-Q. Liang and J.-H. Yu, *Polym. Chem.*, 2017, **8**, 1833; (*b*) J. Li, D.-G. Jia, Z.-J. Guo, Y.-Q. Liu, Y. N. Lyu, Y. Zhou and J. Wang, *Green Chem.*, 2017, **19**, 2675; (*c*) J.-Q. Wang, W. H. Sng, G.-S. Yi and Y.-G. Zhang, *Chem. Commun.*, 2015, **51**, 12076.

18 S. Fischer, J. Schmidt, P. Strauch and A. Thomas, *Angew. Chem., Int. Ed.*, 2013, **52**, 12174.

19 F. Qiu, W.-X. Zhao, S. Han, X.-D. Zhuang, H.-L. Lin and F. Zhang, *Polymers*, 2016, **8**, 1.

20 J. F. Van Humbeck, M. L. Aubrey, A. Alsbaiee, R. Ameloot, G. W. Coates, W. R. Dichtel and J. R. Long, *Chem. Sci.*, 2015, **6**, 5499.

21 Z. Yan, Y. Yuan, Y. Tian, D. Zhang and G. Zhu, *Angew. Chem., Int. Ed.*, 2015, **54**, 12733.

22 S. Ebel, *Arch. Pharm.*, 1968, **4**, 241.

23 A. Trewin, D. J. Willock and A. I. Cooper, *J. Phys. Chem. C*, 2008, **112**(51), 20549.

24 A. Kumar, Ekavali, K. Chopra, M. Mukherjee, R. Pottabathini and D. K. Dhull, *Eur. J. Pharmacol.*, 2015, **761**, 288.